2009 American Control Conference
Hyatt Regency Riverfront, St. Louis, MO, USA
June 10-12, 2009

Fractional-order [Proportional Derivative] Controller for Robust Motion Control: Tuning Procedure and Validation

Ying Luo‡ and YangQuan Chen§

***Abstract*— A fractional-order [proportional derivative] (FO-[PD]) controller is proposed for robust motion control systems. Focusing on a class of simplified models for motion control systems, a practical and systematic tuning procedure has been developed for the proposed FO-[PD] controller synthesis. The fairness issue in comparing with other controllers such as the traditional integer order PID (IO-PID) controller and the fractional order proportional derivative (FO-PD) controller has been for the first time addressed under the same number of design parameters and the same specifications. Side-to-side fair comparisons of the three controllers (i.e., IO-PID, FO-PD and FO-[PD]) via both simulation and experimental tests have revealed some interesting facts: 1) IO-PID controller designed may not always be stabilizing to achieve flat-phase specification while both FO-PD and FO-[PD] controllers designed are always stabilizing; 2) Both FO-PD and FO-[PD] controllers outperform IO-PID controller designed in this paper; 3) FO-[PD] controller outperforms FO-PD controller more when the time constant of the motion control system increases. Extensive validation tests on our real-time experimental test-bench illustrate the same.**

***Index Terms*— Fractional calculus; fractional order controller; motion control; robustness; controller tuning.**

I. Introduction

In recent years, the application of fractional calculus have been attracting more and more researches in science and engineering [1] [2] [3] [4] [5]. Especially, the controllers making use of factional order derivatives and integrals could achieve better performance and robustness results over the conventional integer order controllers [6]. The fractional order PID controller was proposed in [2] as a generalization of PID controller, where the expanding derivatives and integrals to fractional orders can adjust the frequency response of the control system directly and continuously. This great flexibility makes it possible to demonstrate better performance and more robust control in comparison with the traditional PID controller. Reference [7] gives a fractional order PID controller by minimizing the integral of the error squares. Some numerical examples of the fractional order were presented in [8]. However, it is not straightforward to set the parameters of the fractional order controllers in systematic way because of the complexity [9][10][11][8]. Moreover, designing the fractional order PID controller properly and comparing it with the traditional integer order PID controller fairly to illustrate the advantage potential of the fractional calculus is even more complicated. But we may be able to get a practical parameters tuning scheme of fractional order controller for a certain type of simplified motion control systems.

In this paper, a fractional-order [proportional derivative] (FO-[PD]) controller is proposed for robust motion control systems. Focusing on a class of simplified models for motion control systems, a practical and systematic tuning procedure has been developed for the proposed FO-[PD] controller synthesis. The fairness issue in comparing with other controllers such as the traditional integer order PID (IO-PID) controller and the fractional order proportional derivative (FO-PD) [6] controller has been for the first time addressed under the same number of design parameters and the same specifications. Side-to-side fair comparisons of the three controllers (i.e., IO-PID, FO-PD and FO-[PD]) via both simulation and experimental tests have revealed some interesting facts: 1) IO-PID controller designed may not always be stabilizing to achieve flat-phase specification while both FO-PD and FO-[PD] controllers designed are always stabilizing; 2) Both FO-PD and FO-[PD] controllers outperform IO-PID controller designed in this paper; 3) FO-[PD] controller outperforms FO-PD controller more when the time constant of the motion control system increases. Extensive validation tests on our real-time experimental test-bench illustrate the same.

‡Email: ying.luo@ieee.org; Ying Luo is a Ph.D. candidate with the Department of Automation Science and Technology in South China University of Technology, Guangzhou, P.R. China and he was an exchange Ph.D. student at Center for Self-Organizing and Intelligent Systems (CSOIS), Dept. of Electrical and Computer Engineering, Utah State University, Logan, UT, USA from Sept. 2007 to Feb. 2009 under the full financial support from the China Scholarship Council (CSC).

§Corresponding author. Email: yqchen@ieee.org; Tel. 01(435)797-0148; Fax: 01(435)797-3054; Electrical and Computer Engineering Department, Utah State University, Logan, UT 84322, USA. URL: http://fractionalcalculus.googlepages.com/.

II. The Motion control system concerned and the specifications for the three controllers design

A. The Motion Control System Considered

The motion control system focused on in this paper is

$$P(s) = \frac{1}{s(Ts+1)}. \tag{1}$$

which can approximately model a DC motor position servo system. Note that, the plant gain is normalized to 1 without loss of generality since the DC gain of the system concerned can be incorporated in the proportional factor of the controller.

B. The Forms of the Three Controllers Discussed

As we know, the traditional integer order PID controller has the following form of transfer function,

$$C_1(s) = K_{p1}(1 + \frac{K_{i1}}{s} + K_{d1}s). \tag{2}$$

The FO-PD controller has the following transfer function,

$$C_2(s) = K_{p2}(1 + K_{d2}s^{\lambda}), \tag{3}$$

where $\lambda \in (0, 2)$. Clearly, this is a specific form of the most common $PI^{\gamma}D^{\lambda}$ controller which involves an integrator of order γ ($\gamma = 0$, in this paper) and a differentiator of order λ.

The proposed FO-[PD] controller in this paper is defined as the following,

$$C_3(s) = K_{p3}[1 + K_{d3}s]^{\mu}, \tag{4}$$

where $\mu \in (0, 2)$.

C. Three Specifications for the Three Controllers Design

With the motion control system model P(s) in (1) and the generalized form $C(s)$ of the three controllers in II-B, the open-loop transfer function $G(s)$ has the form below,

$$G(s) = C(s)P(s). \tag{5}$$

Here, three specifications to be respectively met by the above three controllers are developed. From the basic definition of gain crossover frequency and phase margin, the following rules can be obtained.

1) Phase margin specification:

$$\begin{aligned} \mathrm{Arg}[G(j\omega_c)] &= \mathrm{Arg}[C(j\omega_c)P(j\omega_c)] \\ &= -\pi + \phi_m, \end{aligned}$$

where ω_c is the gain crossover frequency interested, and ϕ_m is the phase margin required.

2) Robustness to variation in the DC gain of the system:

$$(\frac{\mathrm{d}(\mathrm{Arg}(C(j\omega)P(j\omega)))}{\mathrm{d}\omega})_{\omega=\omega_c} = 0,$$

with the condition that the phase derivative w. r. t. the frequency is zero, i.e., the phase Bode plot is flat, at the gain crossover frequency. It means that the system is more robust to gain changes and the overshoots of the response are almost the same.

3) Gain crossover frequency specification:

$$|G(j\omega_c)|_{dB} = |C(j\omega_c)P(j\omega_c)|_{dB} = 0.$$

III. Integer Order PID Controller Design

In this section, we restrict our attention to the motion control model $P(s)$ described by (1). The IO-PID controller has the form of transfer function in (2). The phase and gain of the plant in frequency domain can be given from (1) by

$$\begin{aligned} \mathrm{Arg}[P(j\omega)] &= -\tan^{-1}(\omega T) - \frac{\pi}{2}, & (6)\\ |P(j\omega)| &= \frac{1}{\omega\sqrt{1+(\omega T)^2}}. & (7) \end{aligned}$$

Integer order PID controller described by (2) can be written as

$$\begin{aligned} C_1(j\omega) &= K_{p1}(1 + K_{i1}\frac{1}{j\omega} + K_{d1}(j\omega)) \\ &= \frac{K_{p1}(K_{i1} - K_{d1}\omega^2) + jK_{p1}\omega}{j\omega}, & (8) \end{aligned}$$

the phase and gain are as follows,

$$\begin{aligned} \mathrm{Arg}[C_1(j\omega)] &= \tan^{-1}(\frac{\omega}{K_{i1} - K_{d1}\omega^2}) - \frac{\pi}{2}, & (9)\\ |C_1(j\omega)| &= \frac{K_{p1}}{\omega}\sqrt{\omega^2 + (K_{i1} - K_{d1}\omega^2)^2}. & (10) \end{aligned}$$

The open-loop transfer function $G_1(s)$ is that

$$G_1(s) = C_1(s)P(s), \quad (11)$$

from (6) and (9), the phase of $G_1(s)$ is as follows,

$$\begin{aligned} &\mathrm{Arg}[G_1(j\omega)] \\ =\ &\tan^{-1}(\frac{\omega}{K_{i1} - K_{d1}\omega^2}) - \tan^{-1}(\omega T) - \pi. \quad (12) \end{aligned}$$

A. Numerical Computation Process

According to Specification II-C.1, the phase of $G_1(s)$ can be expressed as

$$\begin{aligned} &(\mathrm{Arg}[G_1(j\omega)])_{\omega=\omega_c} \\ =\ &\tan^{-1}(\frac{\omega_c}{K_{i1} - K_{d1}\omega_c^2}) - \tan^{-1}(\omega_c T) - \pi \\ =\ &-\pi + \phi_m, & (13) \end{aligned}$$

so, the relationship between K_{d1} and K_{i1} can be established as below,

$$K_{d1} = \frac{K_{i1}}{\omega^2} - \frac{1}{\omega_c \tan(\Phi_m + \tan^{-1}(T\omega_c))}. \quad (14)$$

According to Specification II-C.2 about the robustness to gain variations in the system,

$$\begin{aligned} &(\frac{\mathrm{d}(\mathrm{Arg}(G_1(j\omega)))}{\mathrm{d}\omega})_{\omega=\omega_c} \\ =\ &\frac{K_{d1} - \frac{K_{i1}}{\omega_c^2}}{1 + (\frac{K_{d1}\omega_c^2 - K_{i1}}{\omega_c})^2} - \frac{T}{1+(T\omega_c)^2} \\ =\ &0, & (15) \end{aligned}$$

we can establish another equation about K_d and K_{i1} in the following form,

$$A_1\omega_c^4 K_{d1}^2 - B_1 K_{d1} + C_1 = 0, \quad (16)$$

that is

$$K_{d1} = \frac{B_1 \pm \sqrt{B_1^2 - 4A_1\omega_c^4 C_1}}{2A_1\omega_c^4}, \quad (17)$$

where

$$\begin{aligned} A_1 &= \frac{T}{1+(T\omega_c)^2}, \\ B_1 &= (1 + 2A_1K_{i2})\omega_c^2, \\ C_1 &= A_1\omega_c^2 + A_1K_{i1}^2 - K_{i1}. \end{aligned}$$

According to Specification II-C.3, we can establish an equation about K_i1, K_{d1} and K_{p1},

$$\begin{aligned} |G_1(j\omega_c)| &= |C_1(j\omega_c)||P(j\omega_c)| \\ &= \frac{K_{p1}\sqrt{\omega_c^2 + (K_{i1} - K_{d1}\omega_c^2)^2}}{\omega_c^2\sqrt{1+(T\omega_c)^2}} \\ &= 1. & (18) \end{aligned}$$

Clearly, we can solve equations (14), (17) and (18) to get K_{p1}, K_{d1} and K_{i1}.

B. Tuning Procedure Summary

From the two equations (14) and (17), we can see that it is complicated to get the analytical solution of the parameters K_{d1} and K_{i1}. Fortunately, a graphical method can be used as a practical and simple way to get K_{d1} and K_{i1} because of the plain forms about (14) and (17). The procedure to tune the parameters of the integer order PID controller is as follows:

1) Given ω_c, the gain crossover frequency;
2) Given Φ_m, the desired phase margin;
3) Plot the curve 1, K_{d1} w. r. t K_{i1}, according to (14);
4) Plot the curve 2, K_{d1} w. r. t K_{i1}, according to (17);
5) Obtain the K_{d1} and K_{i1} from the intersection point on the above two curves;
6) Calculate the K_{p1} from (18).

Remark 3.1: The parameters of IO-PID controller designed following the developed procedure may be negative, if so, the closed-loop transfer function will exist a negative characteristic root, thus the system will be unstable using this designed IO-PID controller.

C. Parameters Design Example and Bode Plot Validation of the IO-PID Controller

The motion control system time constant T in (1) is 0.04s, and the specifications of interest are set as $\omega_c = 10(rad./sec.)$, $\Phi_m = 70^o$. According to (14) and (17), two curves are plotted easily to obtain the K_{d1} and K_{i1} from the intersection point, $K_{d1} = 0.1018$ and $K_{i1} = -4.625$. Then K_{p1} can be calculated from (18), that is $K_{p1} = 23.0782$. We can draw the Bode plot to validate that the gain crossover frequency specification $\omega_c = 10(rad/sec)$, phase margin specification $\Phi_m = 70^o$, and the flat-phase specification are all fulfilled. However, when the parameter $K_{i1} = -4.625 < 0$, there will exist a negative characteristic root of the closed-loop transfer function, thus the system using this designed IO-PID controller could be unstable. So, we can not obtain a properly designed IO-PID controller which can guarantee the system stable and achieve the flat-phase specification at the interested gain across frequency.

IV. Fractional Order PD Controller Design

In this section, we also focus on the motion control system model $P(s)$ described by (1). The FO-PD controller has the form of transfer function in (3). The numerical computation process can be seen in [6]. So, the details are omitted except some important equations below.

According to Specification II-C.1, the first relationship between K_d and λ can be established,

$$\begin{aligned} K_{d2} &= \frac{1}{\omega_c^{\lambda}}\tan[\phi+\tan^{-1}(\omega_c T)-\frac{\lambda\pi}{2}+\pi]\cos\frac{(1-\lambda)\pi}{2} \\ &\quad -\frac{1}{\omega_c^{\lambda}}\sin\frac{(1-\lambda)\pi}{2}. \end{aligned} \tag{19}$$

According to Specification II-C.2, we can get the second relationship between K_{d2} and λ in the following form,

$$A_2\omega_c^{2\lambda}K_{d2}^2+B_2K_{d2}+A_2=0, \tag{20}$$

that is,

$$K_{d2}=\frac{-B_2\pm\sqrt{B_2^2-4A_2^2\omega_c^{2\lambda}}}{2A_2\omega_c^{2\lambda}}, \tag{21}$$

where

$$\begin{aligned} A_2 &= \frac{T}{1+(\omega_c T)^2}, \\ B_2 &= 2A_2\omega_c^{\lambda}\sin\frac{(1-\lambda)\pi}{2}-\lambda\omega_c^{\lambda-1}\cos\frac{(1-\lambda)\pi}{2}. \end{aligned}$$

According to Specification II-C.3, we can obtain an equation about K_{p2}, K_{d2} and λ,

$$\begin{aligned} & |G(j\omega_c)| \\ = \; & |C(j\omega_c)||P(j\omega_c)| \\ = \; & \frac{K_{p2}\sqrt{(1+K_{d2}\omega_c^{\lambda}\cos\frac{\lambda\pi}{2})^2+(K_{d2}\omega_c^{\lambda}\sin\frac{\lambda\pi}{2})^2}}{\omega_c\sqrt{1+(\omega_c T)^2}} \\ = \; & 1. \end{aligned} \tag{22}$$

Clearly, we can solve equations (19), (21) and (22) to get λ, K_{d2} and K_{p2}.

A. Design Procedure Summary

The graphical method can also be used as a practical and simple way to get K_{d2} and λ. The procedure of the FO-PD controller tuning is as follows:

1) Given ω_c, the gain crossover frequency;
2) Given Φ_m, the desired phase margin;
3) Plot the curve 1, K_{d2} w. r. t λ, according to (19);
4) Plot the curve 2, K_{d2} w. r. t λ, according to (21);
5) Obtain the K_{d2} and λ from the intersection point on the above two curves;
6) Calculate the K_{p2} from (22).

B. Parameters Design Example and Bode Plot Validation of the FO-PD Controller

The time constant T in (1) is also 0.04s, and the specifications of interest are set as $\omega_c = 10(rad./sec.)$, $\Phi_m = 70^o$. According to (19) and (21), obtain the K_{d2} and λ obviously from the intersection point, that is $K_{d2} = 0.368$ and $\lambda = 0.835$. Then K_{p2} can be calculated from (22), $K_{p2} = 13.8601$.

We can draw the Bode plot to validate that the three specifications in (II-C) are all fulfilled.

V. Fractional Order [PD] Controller Design

In this section, the motion control system model $P(s)$ described by (1) are also considered. The proposed FO-[PD] controller has the transfer function form of (4). The phase and gain of the motion control system model in frequency domain can be given in (6) and (7) respectively.

The FO-[PD] controller described by (4) can be written as

$$C_3(j\omega) = K_{p3}[1+K_{d3}(j\omega)]^{\mu}, \tag{23}$$

The phase and gain are as follows,

$$\begin{aligned} \mathrm{Arg}[C_3(j\omega)] &= \mu\tan^{-1}(\omega K_{d3}), &(24)\\ |C_3(j\omega)| &= K_{p3}[1+(K_{d3}\omega)^2]^{\frac{\mu}{2}}. &(25) \end{aligned}$$

The open-loop transfer function $G_3(s)$ is that

$$G_3(s)=C_3(s)P(s), \tag{26}$$

from (6) and (24), we can get the phase of $G_3(s)$,

$$\begin{aligned} & \mathrm{Arg}[G_3(j\omega)] \\ = \; & \mu\tan^{-1}(\omega K_{d3})-\tan^{-1}(\omega T)-\frac{\pi}{2}. \end{aligned} \tag{27}$$

A. Numerical Computation Process

According to Specification II-C.1, the phase of $G_3(s)$ can be expressed as

$$\begin{aligned} & (\mathrm{Arg}[G_3(j\omega)])_{\omega=\omega_c} \\ = \; & \mu\tan^{-1}(\omega_c K_{d3})-\tan^{-1}(\omega_c T)-\frac{\pi}{2} \\ = \; & -\pi+\phi_m, \end{aligned} \tag{28}$$

from (28), we can establish one relationship between K_{d3} and μ,

$$K_{d3} = \frac{1}{\omega_c}\tan(\frac{1}{\mu}(\Phi_m-\frac{\pi}{2}+\tan^{-1}(T\omega))). \tag{29}$$

According to Specification II-C.2 about the robustness to gain variations in the plant,

$$\begin{aligned} & (\frac{\mathrm{d}(\mathrm{Arg}(G_3(j\omega)))}{\mathrm{d}\omega})_{\omega=\omega_c} \\ = \; & \frac{\mu K_{d3}}{1+(K_{d3}\omega_c)^2}-\frac{T}{1+(T\omega_c)^2} \\ = \; & 0, \end{aligned} \tag{30}$$

another relationship between K_{d3} and μ can be obtained in the following form,

$$A_3\omega_c^2K_{d3}^2-\mu K_{d3}+A_3=0, \tag{31}$$

that is

$$K_{d3}=\frac{\mu\pm\sqrt{\mu^2-4A_3\omega_c^2}}{2A_3\omega_c^2}, \tag{32}$$

where

$$A_3 = \frac{T}{1+(T\omega_c)^2}.$$

According to Specification II-C.3, we can establish an equation about K_{p3}, K_{d3} and μ,

$$\begin{aligned} |G_3(j\omega_c)| &= |C_3(j\omega_c)||P(j\omega_c)| \\ &= \frac{\sqrt{(T\omega_c^2)^2+\omega_c^2}}{(1+(K_{d3}\omega_c)^2)^{\frac{\mu}{2}}} \\ &= 1. \end{aligned} \tag{33}$$

Clearly, we can solve equations (29), (32) and (33) to get K_{p3}, K_{d3} and μ.

B. Design Procedure Summary

The graphical method can be also used as a practical and simple way to get K_{d3} and μ. The procedure to tune the parameters of the FO-[PD] controller is as follows:

1) Given ω_c, the gain crossover frequency;
2) Given Φ_m, the desired phase margin;
3) Plot the curve 1, K_{d3} w. r. t μ, according to (29);
4) Plot the curve 2, K_{d3} w. r. t μ, according to (32);
5) Obtain the K_{d3} and μ from the intersection point on the above two curves;
6) Calculate the K_{p3} from (33).

C. Parameters Design Example and Bode Plot Validation of the FO-[PD] Controller

The time constant T in (1) is 0.04s, and the specifications of interest are also set as $\omega_c = 10(rad./sec.)$, $\Phi_m = 70^o$. According to (29) and (32), two curves are plotted easily to obtain the K_{d3} and μ from the intersection point, $K_{d3} = 0.2991$ and $\mu = 0.7825$. Then K_{p3} can be calculated from (33), that is $K_{p3} = 16.7839$.

Again, we can draw the Bode plot to validate that the gain crossover frequency specification, $\omega_c = 10(rad/sec)$, and phase margin specification, $\Phi_m = 70^o$, are fulfilled, and the phase is forced to be flat at ω_c.

VI. Implementation of two Fractional Order Operators for the two Fractional Order Controllers

In this paper, the fractional order operators s^λ for the FO-PD controller and $(1+\tau s)^\mu$ for the FO-[PD] controller are implemented by the impulse response invariant discretization methods in time domain.

A. Implementation of s^λ for FO-PD Controller

In [6], the fractional order operator s^λ in (3) for the FO-PD controller is implemented by the frequency domain approximation method with the Oustaloup Recursive Algorithm [12], which is a band-limit finite dimensional approximation, and a proper range of frequency of practical interest is needed. In this paper, s^λ is realized by the Impulse Response Invariant Discretization (IRID) method [13] in time domain, where a discrete-time finite dimensional (z) transfer function is computed to approximate the continuous irrational transfer function s^λ, s is the Laplace transform variable, and λ is a real number in the range of (-1,1). s^λ is called a fractional order differentiator if $0 < \lambda < 1$ and a fractional order integrator if $-1 < \lambda < 0$. This approximation keeps the impulse response invariant.

B. Implementation of $(1 + \tau s)^\mu$ for FO-[PD] Controller

The proposed fractional order operator $(1 + \tau)s)^\mu$ in (4) for the FO-[PD] controller is implemented by modifying the code of the IRID of fractional order low-pass filters (IRID-FOLPF) [14]. In the code of IRID-FOLPF, a discrete-time finite dimensional (z) transfer function is computed to approximate a continuous-time fractional order low-pass filter (LPF) $[1/(\tau s+1)]^{\mu'}$, s is the Laplace transform variable, and μ' is a real number in the range of (0,1), τ is the time constant of LPF. This approximation also keeps the impulse response invariant and only supports when μ' in (0,1). That is the fractional order low pass filter.

When μ' is in (-1,0), $[1/(\tau s + 1)]^{\mu'}$ is just the fractional order operator for the FO-[PD] controller. The implementation of this operator $[1/(\tau s + 1)]^{\mu'}$ is realized as follows. First, FO-LPF $[1/(\tau s + 1)]^{-\mu'}$ ($\mu' \in (-1, 0)$) is realized via the IRID-FOLPF introduced above, we can obtain the discretized transfer function of the FO-LPF,

$$G_{FO-LPF} = \frac{A(z)}{B(z)}.$$

Then, FO-[PD] operator $[1/(\tau s+1)]^{\mu'}$=$(\tau s+1)^\mu$ ($\mu \in (0, 1)$) can be obtained,

$$G_{FO-[PD]} = \frac{B(z)}{A(z)},$$

where $G_{FO-[PD]}$ is the discretized transfer function of the FO-[PD] operator.

VII. Simulation

The tuning procedures above for the three controllers are illustrated via numerical simulation in this section.

In order to compare the IO-PID controller, FO-PD controller and the proposed FO-[PD] controller fairly, two simulation cases are presented.

A. Step Response Comparison Using the Three Controllers with the Motion Control System Time Constant $T = 0.4$

In the case, the motion control system time constant T in (1) is 0.4s. The specifications of interest are set as $\omega_c = 10(rad./sec.)$, $\Phi_m = 70^o$, and the robustness to gain variations in the system is required.

The parameters of the IO-PID, FO-PD and FO-[PD] controllers are already calculated in the examples of sections III-C, IV-B and V-C respectively.

In Fig. 1, applying the FO-PD controller, the unit step responses are plotted with the open-loop plant gain varying from 11.0881 to 16.6321 ($\pm 20\%$ variations from the desired value 13.8601). In Fig. 2, applying FO-[PD] controller, the unit step responses are plotted with open-loop gains changing from 13.4271 to 20.1407 ($\pm 20\%$ variations from desired value 16.7839).

It can be seen from Fig. 1 and Fig. 2 that the both the FO-PD and the FO-[PD] controllers designed following the proposed method in this paper are effective. The overshoots of the step responses remain almost constant under gain variations, i.e. the iso-damping property is exhibited, that means the system is robust to gain changes. Furthermore, from Fig. 3, it can be seen obviously that the over shoot of the red line with the proposed FO-[PD] controller is smaller then that of the blue line with the FO-PD controller. So, we can see the FO-[PD] controller outperforms the FO-PD controller.

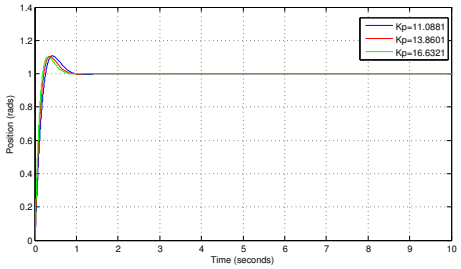

Fig. 1. Simulation. Step responses with FO-PD controller (T=0.4)

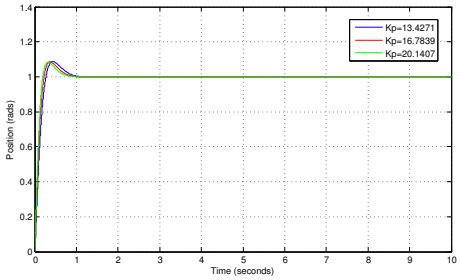

Fig. 2. Simulation. Step responses with FO-[PD] controller (T=0.4)

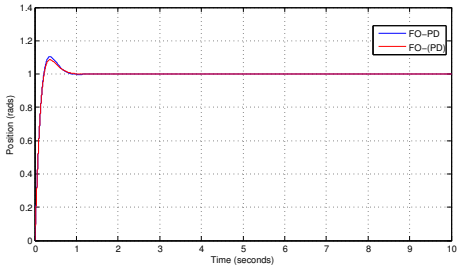

Fig. 3. Simulation. Step responses comparison with two FO controllers (T=0.4)

B. Step Response Comparison Using the Three Controllers with the Motion Control System Time Constant $T = 0.04$

In the case, the motion control system time constant T in (1) is 0.04s. The specifications of interest are set as $\omega_c = 10(rad./sec.)$, $\Phi_m = 70^o$, and the robustness to gain variations in the system is also required.

1) Parameters design for the three controllers: Following the tuning procedure summary in (III-B), we can get the three parameter values of the IO-PID controller, $K_{d1} = 0.0189$, $K_{i1} = 1.5670$ and $K_{p1} = 10.7649$. In this case, as the three parameters K_{d1}, K_{i1} and K_{p1} are all positive, so, this designed IO-PID controller can guarantee the system stable and satisfy the three specifications in (II-C) at the same time.

According to the tuning procedure summaries in (IV-A) and (V-B), we can get the three parameter values of the FO-PD controller, $K_{d2} = 0.0057$, $\lambda = 0.7796$, $K_{p2} = 10.6417$, and the three parameter values of the FO-[PD] controller, $K_{d2} = 0.0057$, $\lambda = 0.7796$, $K_{p2} = 10.6417$, respectively.

2) Step responses comparison: In Fig. 4, applying the IO-PID controller, the unit step responses are plotted with the open-loop plant gain varying from 8.6199 to 12.9179 ($\pm 20\%$ variations from the desired value 10.7649). In Fig. 5, applying the FO-PD controller, the unit step responses are plotted with the open-loop plant gain varying from 8.5134 to 12.7701 ($\pm 20\%$ variations from the desired value 10.6417). And in Fig. 6, applying FO-[PD] controller, the unit step responses are plotted with open-loop gains changing from 8.6082 to 12.9124 ($\pm 20\%$ variations from desired value 10.7603).

It can be seen from Fig. 4, Fig. 5 and Fig. 6 that the IO-PID controller designed following the procedure in III does work, the overshoot just changes almost 1.2% as the open-loop plant gain varies 20%. From Fig. 5 and Fig. 6, we can see that, the step responses using the FO-PD and FO-[PD] controllers almost have no overshoot, even the open-loop plant gains vary 20%. So the iso-damping property is exhibited adequately, the robustness of the system using the FO-PD and FO-[PD] controllers is better than that using the IO-PID controller. Furthermore, from Fig. 3, it can be seen obviously that, the performance using both of the FO-PD and FO-[PD] controllers are much better than the IO-PID controller which is designed by the same specifications with the FO-PD and FO-[PD] controllers.

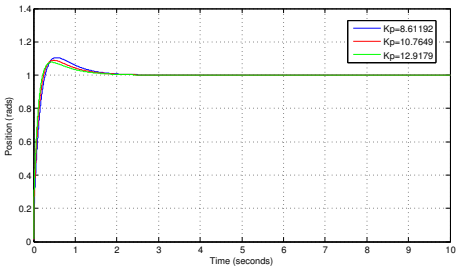

Fig. 4. Simulation. Step responses with IO-PID controller (T=0.04)

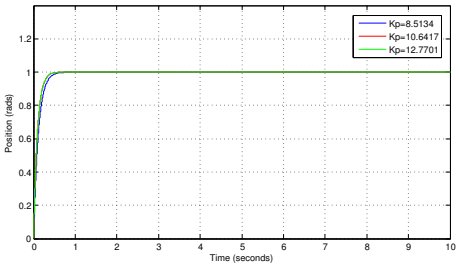

Fig. 5. Simulation. Step responses with FO-PD controller (T=0.04)

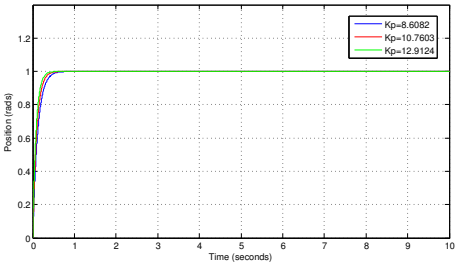

Fig. 6. Simulation. Step responses with FO-[PD] controller (T=0.04)

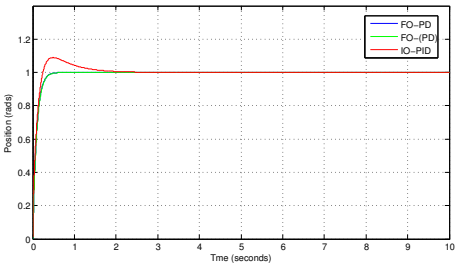

Fig. 7. Simulation. Step responses comparison with three controllers (T=0.04)

VIII. Experiment

A. Introduction of the Experimental Platform

A fractional horsepower dynamometer was developed as a general purpose experiment platform [15]. The architecture of the dynamometer control system is shown in Fig. 8. The dynamometer includes the DC motor to be tested, a hysteresis brake for applying torque load to the motor, a load cell to provide force feedback, an optical encoder for position feedback and a tachometer for velocity feedback. The dynamometer was modified to connect to a Quanser MultiQ4 terminal board in order to control the system through Matlab/Simulink Real-Time Workshop (RTW) based software. This terminal board connects with the Quanser MultiQ4 data acquisition card. Then, use the Matlab/Simulink environment, which uses the WinCon application from Quanser, to communicate with the data acquisition card. This enables rapid prototyping and experiment capabilities.

Without loss of generality, consider the motion control system modeled by:

$$\dot{x}(t) = v(t), \tag{34}$$

$$\dot{v}(t) = K_u u(t) - K_b v. \tag{35}$$

where x is the position state, v is the velocity, and u is the control input, K_u and K_b are positive coefficients.

Through simple system identification process, the DC motor velocity control system can be approximately modeled by a simple first order transfer function $\frac{1.52}{0.4s+1}$.

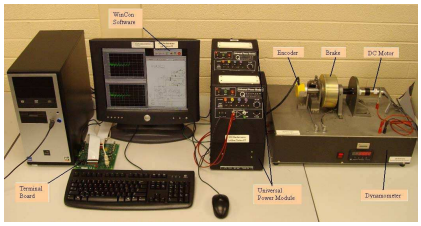

Fig. 8. The dynamometer setup

B. Experiments on the Dynamometer

Since we already have experimentally modeled the velocity control system of the dynamometer with a transfer function $\frac{1.52}{0.4s+1}$, the position control system of the dynamometer has the same structure of the motion control system model (1). Thus, the simulation results in VII-A with the motion control system time constant $T = 0.4$ can be validated via the real-time experiments on the dynamometer.

In Fig. 9, applying the FO-PD controller, the unit step responses are plotted with the open-loop plant gain varying from 11.0881 to 16.6321 ($\pm 20\%$ variations from the desired value 13.8601). In Fig. 10, applying FO-[PD] controller, the unit step responses are plotted with open-loop gains changing from 13.4271 to 20.1407 ($\pm 20\%$ variations from desired value 16.7839).

It can be seen from Fig. 9 and Fig. 10 that the both of the FO-PD and FO-[PD] controllers designed by the proposed method in this paper are effective. The overshoots of the step responses remain almost constant under gain variations, the systems are robust to gain changes. Furthermore, from Fig. 11, it can be seen obviously that the over shoot of the red line with the proposed FO-[PD] controller is smaller than that of the blue line with the FO-PD controller. So, we can see the FO-[PD] controller outperforms the FO-PD controller.

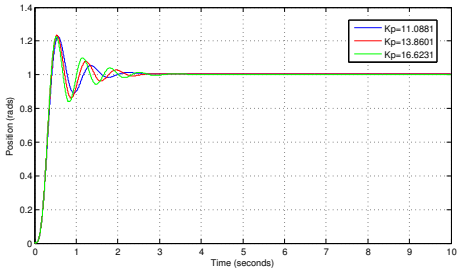

Fig. 9. Experiment. Step responses with FO-PD controller

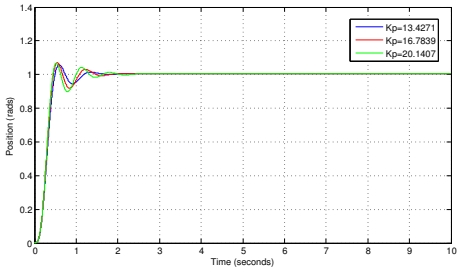

Fig. 10. Experiment. Step responses with FO-[PD] controller

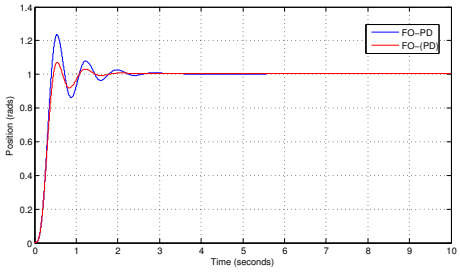

Fig. 11. Experiment. Step responses comparison with two controllers

IX. Conclusions

In this paper, a new fractional-order [proportional derivative] (FO-[PD]) controller is proposed for robust motion control systems. Focusing on a class of simplified models for motion control systems, a practical and systematic tuning procedure has been developed for the proposed FO-[PD] controller synthesis. The fairness issue in comparing with other controllers such as the traditional integer order PID (IO-PID) controller and the fractional order proportional derivative (FO-PD) controller has been for the first time addressed under the same number of design parameters and the same specifications. Side-to-side fair comparisons of the three controllers (i.e., IO-PID, FO-PD and FO-[PD]) via both simulation and experimental tests have revealed some interesting facts: 1) IO-PID designed may not always be stabilizing to achieve flat-phase specification while both FO-PD and FO-[PD] designed are always stabilizing; 2) Both FO-PD and FO-[PD] outperform IO-PID designed in this paper; 3) FO-[PD] outperforms FO-PD more when the time constant of the motion control system increases. Extensive validation tests on our real-time experimental test-bench illustrate the same.

References

[1] K. S. Miller and B. Ross, "An introduction to the fractional calculus and fractional differential equations," Wiley, New York, 1993.

[2] I. Podlubny, "Fractional-order systems and $PI^{\lambda}D^{\mu}$ controller," *IEEE Trans. Automatic control*, vol. 44, no. 1, pp. 208–214, 1999.

[3] D. Xue and Y. Q. Chen, "A comparative introduction of four fractional order controllers," in *Proc. of 4th IEEE World Congress on Intelligent Controllers and Automation (WCICA02)*, Shanghai, China, 2002, pp. 3228–3235.

[4] A. Oustaloup, X. Moreau, and M. Nouillant, "The CRONE suspension," *Control Engineering Practice*, vol. 4, no. 8, pp. 1101–1108, 1996.

[5] D. Valerio and J. S. da Costa, "Time-domai implementatio of fractional order controllers," *IEE Proceedings - Control Theory and Applications*, vol. 152, no. 5, pp. 539–552, 2005.

[6] HongSheng Li Ying Luo and YangQuan Chen, "A fractional order proportional and derivative (FOPD) motion controller: Tuning rule and experiments," *IEEE Transactions on Control System Technology (submitted)*.

[7] Z. F. Lv, "Time-domain simulation and design of SISO feedback control systems," *Doctoral Dissertation, National Cheng Kung University*, 2004.

[8] Chunna Zhao, D. Xue, and Y. Q. Chen, "A fractional order PID tuning algorithm for a class of fractional order plants," in *Proc. of the ICMA*, Niagara, Canada, 2005, pp. 216–221.

[9] D. Xue, Chunna Zhao, and Y. Q. Chen, "Fractional order PID control of a dc-motor with elatic shaft: A case study," in *Proc. of American Control Conference(ACC) 2006*, Minnesota, USA, 2006, pp. 3182–3187.

[10] Ziegler, J. G., and N. B. Nichols, "Optimum settings for automatic controllers," *Transactions of the A.S.M.E.*, pp. 759–768, 1942.

[11] C. A. Monje, B. M. Vinagre, Y. Q. Chen, and V. Feliu, "Proposals for fractional $PI^{\lambda}D^{\mu}$-tuning," in *Proceedings of The First IFAC Symposium on Fractional Differentiation and its Applications (FDA04)*, Bordeaux, France, 2004.

[12] A. Oustaloup, J. Sabatier, and P. Lanusse, "From fractional robustness to CRONE control," *Fractional Calculus and Applied Analysis*, vol. 2, no. 1, pp. 1–30, 1999.

[13] YangQuan Chen, "Impulse response invariant discretization of fractional order integrators/differentiators compute a discrete-time finite dimensional (z) transfer function to approximate s^r with r a real number," *Category: Filter Design and Analysis, MATLAB Central, http://www.mathworks.com/matlabcentral/fileexchange/ loadFile.do objectId=21342 objectType=FILE*, 2008.

[14] YangQuan Chen, "Impulse response invariant discretization of fractional order low-pass filters discretize $[1/(\tau s + 1)]^r$ with r a real number," *Category: Filter Design and Analysis, MATLAB Central,http://www.mathworks.com/matlabcentral/fileexchange/ loadFile.do objectId=21365 objectType=FILE*, 2008.

[15] Y. Tarte, YangQuan Chen, Wei Ren, and K. Moore, "Fractional horsepower dynamometer - a general purpose hardware-in-the-loop real-time simulation platform for nonlinear control research and education," in *Proceedings of IEEE Conference on Decision and Control*, 13-15 Dec. 2006, pp. 3912–3917.